

# Mutational Analysis of 48G7 Reveals that Somatic Hypermutation Affects Both Antibody Stability and Binding Affinity

Sophie B. Sun,<sup>†</sup> Shiladitya Sen,<sup>§</sup> Nam-Jung Kim,<sup>†</sup> Thomas J. Magliery,<sup>\*,§</sup> Peter G. Schultz,<sup>\*,†</sup> and Feng Wang<sup>\*,‡</sup>

<sup>†</sup>Department of Chemistry and the Skaggs Institute for Chemical Biology, The Scripps Research Institute, 10550 North Torrey Pines Road, La Jolla, California 92037, United States

<sup>‡</sup>California Institute for Biomedical Research, 11119 North Torrey Pines Road Suite 100, La Jolla, California 92037, United States

<sup>§</sup>Department of Chemistry and Biochemistry, The Ohio State University, 100 West 18th Avenue, Columbus, Ohio 43210, United States

## Supporting Information

**ABSTRACT:** The monoclonal antibody 48G7 differs from its germline precursor by 10 somatic mutations, a number of which appear to be functionally silent. We analyzed the effects of individual somatic mutations and combinations thereof on both antibody binding affinity and thermal stability. Individual somatic mutations that enhance binding affinity to hapten decrease the stability of the germline antibody; combining these binding mutations produced a mutant with high affinity for hapten but exceptionally low stability. Adding back each of the remaining somatic mutations restored thermal stability. These results, in conjunction with recently published studies, suggest an expanded role for somatic hypermutation in which both binding affinity and stability are optimized during clonal selection.

The immune system produces high-affinity, selective antibodies through a process that involves recombination of large numbers of variable (V), diversity (D), and joining (J) gene segments to generate a diverse germline antibody repertoire.<sup>1–3</sup> Subsequent somatic hypermutation of the germline variable domains, together with B cell clonal selection, leads to high-affinity antibodies, a process termed affinity maturation. Point mutations in the complementarity determining regions (CDRs) of the antibody that arise during affinity maturation have historically been associated with increased affinity for antigens.<sup>4</sup> Some of these mutations affect affinity through direct interactions with antigen, and some increase affinity by fixing the conformational plasticity of the germline antigen binding site.<sup>5–8</sup> However, other mutations are distant from bound antigen and have no effect on antigen binding. Recently, we showed that in the case of the antibodies OKT3 and 93F3, which bind protein and small-molecule antigens, respectively, these apparently neutral somatic mutations lead to enhanced antibody thermodynamic stability, compensating for the deleterious effects of affinity mutations on antibody stability.<sup>9</sup> To further explore the generality of this notion, we investigated the role of somatic mutations in the biochemically and structurally well-characterized monoclonal antibody 48G7.<sup>6,10–13</sup> 48G7 is a hydrolytic antibody that was generated

against a *p*-nitrophenylphosphonate transition-state analogue, JWJ1 (Figure 1).<sup>14</sup> Affinity maturation of the germline

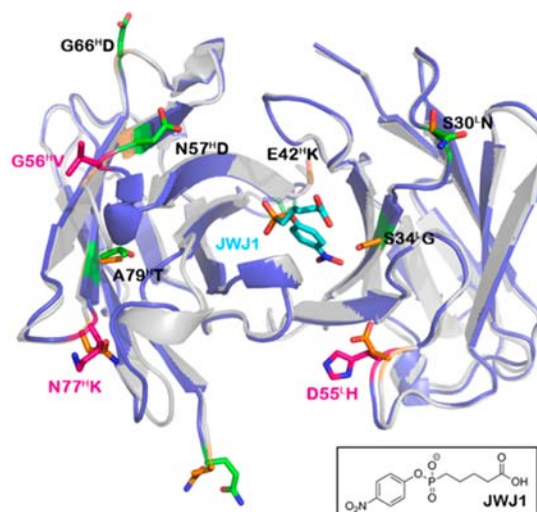


**Figure 1.** Alignment of germline 48G7g structure (gray, PDB code: 1AJ7) with matured 48G7 (blue, PDB code: 1GAF). Somatic mutations involved in binding are highlighted in pink (G56<sup>H</sup>V, N77<sup>H</sup>K, and D55<sup>L</sup>H). The remaining mutations are denoted in green (E1<sup>H</sup>Q, E42<sup>H</sup>K, N57<sup>H</sup>D, G66<sup>H</sup>D, A79<sup>H</sup>T, S30<sup>L</sup>N, and S34<sup>L</sup>G). The corresponding residues in the germline structure are denoted in orange. JWJ1 is shown in its high-affinity binding conformation (cyan) with its chemical structure included below.

precursor to 48G7 resulted in 10 somatic mutations, which decreased the dissociation constant ( $K_D$ ) for the hapten from  $4.8 \times 10^{-5}$  M to  $1.6 \times 10^{-8}$  M, a 3000-fold increase in affinity.<sup>11</sup> A comparison of the X-ray crystal structures of the germline and affinity-matured antibodies shows that most of the somatic mutations are outside of the antigen binding site, up to 15 Å away from the bound hapten.<sup>6,10,13</sup> A number of these mutations were shown to enhance affinity by restricting the conformational plasticity of the antigen binding site.<sup>6</sup> A number of others appeared to be functionally neutral with respect to

Received: March 22, 2013

Published: June 24, 2013

affinity. Here, we show that this latter set of somatic mutations increases the thermal stability of 48G7, suggesting a more general role for the affinity maturation process in which somatic hypermutation and clonal selection function to enhance both antibody affinity and stability.

To determine the effects of individual somatic mutations on antibody stability, we first added individual somatic mutations to the germline precursor 48G7g (E1<sup>H</sup>Q, E42<sup>H</sup>K, G56<sup>H</sup>V, N57<sup>H</sup>D, G66<sup>H</sup>D, N77<sup>H</sup>K, A79<sup>H</sup>T; S30<sup>L</sup>N, S34<sup>L</sup>G, D55<sup>L</sup>H) as well as germline reversion mutations to affinity-matured 48G7 (Q1<sup>H</sup>E, K42<sup>H</sup>E, V56<sup>H</sup>G, D57<sup>H</sup>N, D66<sup>H</sup>G, K77<sup>H</sup>N, T79<sup>H</sup>A; N30<sup>L</sup>S, G34<sup>L</sup>S, H55<sup>L</sup>D) (Figure S3, Supporting Information). All Fab variants were fused to a hexahistidine tag at the C-terminus of the heavy chain, expressed in Freestyle 293 cells, and purified by Ni-NTA affinity chromatography (Supporting Information). The thermal stability of each purified mutant Fab was compared to those of the germline and mature Fabs using differential scanning fluorimetry (DSF) with SYPRO orange dye first in the absence of hapten.<sup>15</sup> We also confirmed  $T_m$  values by comparing DSF versus differential scanning calorimetry measurements for a few key mutants (Figure S4, Supporting Information).

We found that the melting temperature of 48G7 ( $T_m = 63.5$  °C) was 7.0 °C lower than for 48G7g ( $T_m = 70.5$  °C) and that all of the individual mutants fell somewhere within this range (Figures 2, S5A–B; Table S1, Supporting Information). The

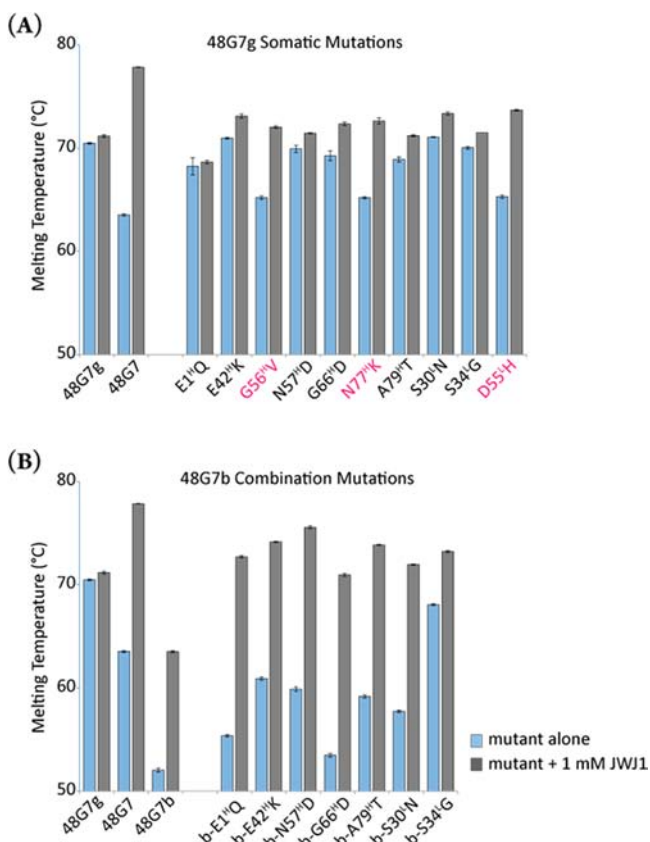


**Figure 2.** Melting temperatures of 48G7 variants in the absence and presence of 1 mM hapten JWJ1: (A) single somatic mutations added to 48G7g and (B) single mutations added to 48G7b (binding mutant: G56<sup>H</sup>V/N77<sup>H</sup>K/D55<sup>L</sup>H). The three mutations that decrease the  $T_m$  of 48G7g the most are highlighted in red. Measurements were repeated twice for these mutants; error bars represent standard error.

addition of G56<sup>H</sup>V, N77<sup>H</sup>K, or D55<sup>L</sup>H to 48G7g decreased the  $T_m$  by more than 5.2 °C, whereas two of the reversion mutations (V56<sup>H</sup>G and D55<sup>L</sup>H) correspondingly increased the  $T_m$  of the mature Fab. K77<sup>H</sup>N introduces a glycosylation site that probably perturbs the local structure, preventing an increase in  $T_m$  (Table S1, Supporting Information).<sup>16</sup> Interestingly, the G56<sup>H</sup>V, N77<sup>H</sup>K, and D55<sup>L</sup>H mutations were previously found to have the greatest effect on the binding affinity of 48G7 for JWJ1, despite the fact that none of these three residues comes into direct contact with JWJ1.<sup>11</sup> Their role in binding most likely involves fixing the conformation of the active site to maximize its complementarity to hapten. The binding affinity of the double mutant N77<sup>H</sup>K/D55<sup>L</sup>H was reported to be  $1.2 \times 10^{-7}$  M, a 400-fold increase over 48G7g.<sup>11</sup> We found that the  $T_m$  of this double mutant was 61.4 °C, 9.1 °C lower than the germline precursor (Table S1, Supporting Information). We next added all three binding mutations to 48G7g in combination (G56<sup>H</sup>V, N77<sup>H</sup>K, D55<sup>L</sup>H; designated as 48G7b) and determined the binding affinity for this and other mutants by biolayer interferometry using the ForteBio OctetRED system with a previously described protocol (Table S2, Supporting Information).<sup>17</sup> 48G7b had an even higher affinity for JWJ1 ( $K_D = 2.9 \times 10^{-8}$  M), close to that of the affinity matured antibody ( $K_D = 1.1 \times 10^{-8}$  M), and a correspondingly greater decrease of 18.5 °C in thermal stability ( $T_m = 52.0$  °C), the lowest of any mutant tested. These results are consistent with the previously reported observation that somatic mutations which lead to significant increases in germline antibody affinity generally result in decreased antibody stability relative to the germline precursor.<sup>9</sup>

Because 48G7b, which has just three somatic mutations, binds hapten with only 3-fold lower affinity than 48G7 and has the lowest stability of all mutants tested, we used it as a scaffold to assess the role of the remaining seven somatic mutations on both thermal stability and binding affinity. We introduced each of the seven remaining “nonbinding” somatic mutations individually into 48G7b (E1<sup>H</sup>Q, E42<sup>H</sup>K, N57<sup>H</sup>D, G66<sup>H</sup>D, A79<sup>H</sup>T; S30<sup>L</sup>N, S34<sup>L</sup>G). All of the somatic mutations increased  $T_m$ , and some had a large impact on  $T_m$ . For example, the S30<sup>L</sup>N, E42<sup>H</sup>K, N57<sup>H</sup>D, and A79<sup>H</sup>T mutations increased the  $T_m$  of 48G7b by 5–9 °C, and the S34<sup>L</sup>G mutation increased the  $T_m$  by 16.1 °C to 68.1 °C, which is even higher than that of 48G7 itself (Table S1, Supporting Information). As expected, the addition of the individual nonbinding somatic mutations had relatively little effect on binding affinity, with the  $K_D$  varying by less than 3-fold from that of 48G7b for each mutant (Table S2, Supporting Information). Taken together, these results indicate that somatic mutations that have relatively little effect on affinity have significant effects on stability, again consistent with the previous studies of antibodies 93F3 and OKT3.<sup>9</sup>

Next, we explored interactions between somatic mutations by combining the mutations as sets. Heavy-chain somatic mutations N57<sup>H</sup>D and A79<sup>H</sup>T are in close proximity to G56<sup>H</sup>V and N77<sup>H</sup>K, respectively. When added together to 48G7b, these mutations led to a 10.5 °C increase in  $T_m$  to 62.5 °C, again with little effect on affinity (Table S2, Supporting Information). However, further introduction of the light chain somatic mutation S30<sup>L</sup>N, which is stabilizing in the context of 48G7b, significantly decreased both  $T_m$  and affinity ( $T_m = 48.7$  °C;  $K_D = 1.6 \times 10^{-7}$  M). Affinity and stability were restored ( $T_m = 61.6$  °C;  $K_D = 3.9 \times 10^{-8}$  M) with the additional somatic mutation S34<sup>L</sup>G, which results in the mature light chain. Thus,

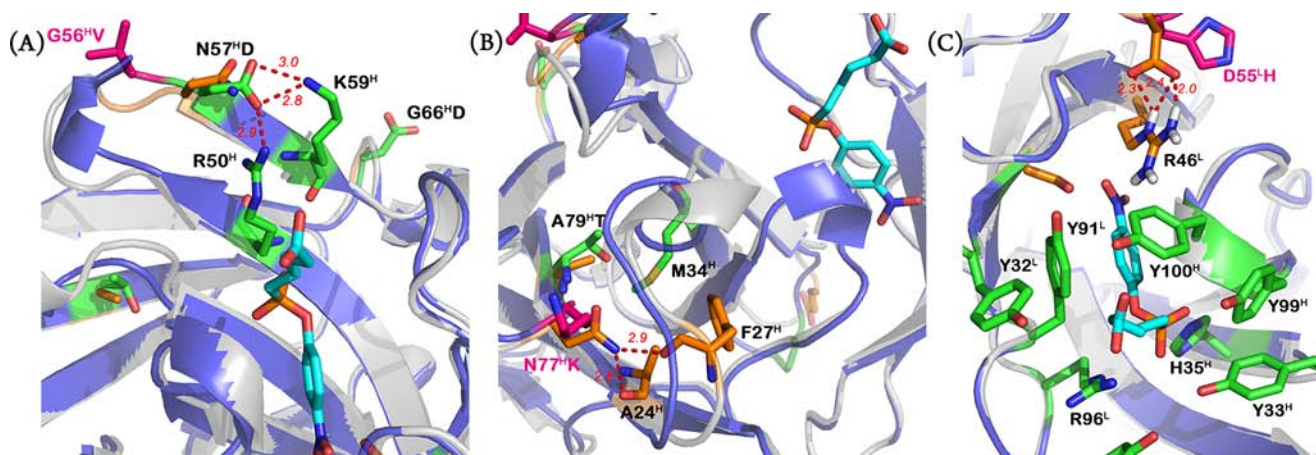


**Figure 3.** Close-up views of key interactions: (A) Somatic mutation N57<sup>H</sup>D introduces hydrogen-bonding interactions with residues R50<sup>H</sup> and K59<sup>H</sup>. (B) Somatic mutation N77<sup>H</sup>K results in the loss of two hydrogen bonds with residues A24<sup>H</sup> and F27<sup>H</sup> in the germline structure. The somatic mutation A79<sup>H</sup>T enhances hydrophobic interactions with M34<sup>H</sup>. (C) Hydrophobic linker of JWJ1 is surrounded by four key tyrosine residues (Y32<sup>L</sup>, Y91<sup>L</sup>, Y99<sup>H</sup>, and Y100<sup>H</sup>). Within this hydrophobic pocket lie H35<sup>H</sup> and R96<sup>L</sup>, which form an oxyanion hole in which binds the phosphonate group. Mutation D55<sup>L</sup>H removes hydrogen-bonding interactions with R46<sup>L</sup>.

the effects of individual somatic mutations appear to be context-dependent versus additive in nature. Indeed, 48G7b-S34<sup>L</sup>G, which contains only four somatic mutations, has significantly higher affinity and thermal stability than 48G7 itself in the absence of JWJ1.

The X-ray crystal structures of 48G7 and its germline precursor provide insights into the structural basis for the effects of somatic mutations on affinity and stability. Previous studies showed that JWJ1 induces a significant conformational change upon binding 48G7g. In contrast, the hapten binds the affinity-matured antibody in a lock-and-key fashion.<sup>6,10,11</sup> None of the three binding mutations (G56<sup>H</sup>V, N77<sup>H</sup>K, and D55<sup>L</sup>H) comes in direct contact with the hapten (Figures 1, 3). The JWJ1 phosphonate group interacts with H35<sup>H</sup> and R96<sup>L</sup> in both 48G7 and the germline precursor, and it forms an additional hydrogen bond with Y33<sup>H</sup> in 48G7, which does not exist in the germline structure. The combined interactions of G56<sup>H</sup>V and N77<sup>H</sup>K with the heavy-chain CDR1 loop may result in improved contacts between Y33<sup>H</sup> and H35<sup>H</sup> and the phosphonate. G56<sup>H</sup>V appears to induce a noncanonical turn that affects packing at the base of the CDR1 loop. However, the twist formed in the loop spanning residues 52<sup>H</sup>-56<sup>H</sup> likely introduces conformational strain that results in a 5.1 °C decrease in the  $T_m$  of 48G7g. The addition of N57<sup>H</sup>D to the G56<sup>H</sup>V mutant introduces hydrogen-bonding interactions with residues R50<sup>H</sup> and K59<sup>H</sup> and a compensating increase in stability ( $\Delta T_m = +3.7$  °C) (Figure 3A). Although the N77<sup>H</sup>K mutation enhances affinity, it results in the loss of two hydrogen bonds to the carbonyl oxygens of A24<sup>H</sup> and F27<sup>H</sup>, reducing the  $T_m$  by 5.3 °C. Introduction of the A79<sup>H</sup>T mutation appears to form a compensating stabilizing hydrophobic interaction with M34<sup>H</sup> and increases  $T_m$  by 2.3 °C (Figure 3B). D55<sup>L</sup>H removes hydrogen-bonding interactions with R46<sup>L</sup>, likely shifting the arginine side chain to allow the high-affinity binding conformation of the hapten (Figure 3C). However, the loss of this salt bridge reduces the thermal stability by 5.2 °C from the germline  $T_m$ . The S34<sup>L</sup>G mutation seems to prevent a steric clash between 48G7 and the JWJ1 nitro group. In the context of 48G7b, S34<sup>L</sup>G significantly increases the thermal stability ( $\Delta T_m = +16.1$  °C), but when S34<sup>L</sup>G is added to 48G7b-N57<sup>H</sup>D/A79<sup>H</sup>T, the  $T_m$  drops by 5.8

°C. Since residue 34<sup>L</sup> is located at the V<sub>H</sub>-V<sub>L</sub> interface, this mutation likely affects surface contacts between the heavy and light chains, which may be different in the context of specific somatic mutations (Figure 1). Unfortunately, it is difficult to recapitulate the immunological evolution path of 48G7 from 48G7g to determine the precise interactions that lead to both affinity and stability maturation.

Next, we determined the effects of hapten binding on the thermal stabilities of 48G7, 48G7g, and a subset of somatic mutations to 48G7g and 48G7b by thermal denaturation of the Fabs in the presence of 1 mM JWJ1 (Figure 2). This concentration of hapten is significantly higher than even the highest  $K_D$  for any 48G7 variant ( $4.6 \times 10^{-5}$  M for 48G7g), ensuring saturation of the binding sites for all mutants.<sup>11</sup> There was relatively little effect of hapten binding on the germline antibody, consistent with the low affinity and high intrinsic stability of the germline repertoire. Similarly, hapten had a relatively small effect on individual somatic mutants of the germline antibody that are not involved in binding. In contrast, addition of hapten to 48G7 led to significant stabilization (above that of the germline antibody). In addition, each of the individual binding somatic mutations (D55<sup>L</sup>H, G56<sup>H</sup>V, and N77<sup>H</sup>K) in the context of 48G7g was stabilized by >6.8 °C upon addition of hapten (Figure 2). Similarly, 48G7b itself showed a significant increase in  $T_m$  (+11.5 °C) in the presence of hapten as did the other 48G7b variants (Table S1, Supporting Information). Thus, it appears that mutations that affect binding are destabilizing, but significantly less so in the presence of hapten. Complementary electrostatic and van der Waals interactions between hapten and antibody likely compensate for the detrimental effects of affinity mutations on stability that are observed in the absence of hapten (Figure 3C). Furthermore, the decreased plasticity of the affinity-matured antibody likely makes it less able to reorganize to accommodate solvent in the unbound state. Then what is the basis for the selection of stabilizing somatic mutations if in the presence of hapten they all have relatively high  $T_m$ s? Previously, we showed that the stability of the antibody correlates with its expression levels in mammalian cells.<sup>9</sup> This suggests that the more stable antibodies will be expressed at higher density on the B cell surface and clonally selected due to higher avidity in

the presence of bound antigen. Studies with OKT3 and 93F3 support these conclusions, implying that thermal stability may lead to improved expression levels and avidity.<sup>9</sup>

Through detailed mutational analysis of 48G7 and its germline precursor, we have obtained a better understanding of how somatic hypermutation influences both antibody stability and binding affinity. While binding mutations (D55<sup>L</sup>H, G56<sup>H</sup>V, N77<sup>H</sup>K) result in decreased  $T_m$ , other mutations arise to restore thermal stability (Figure 4).

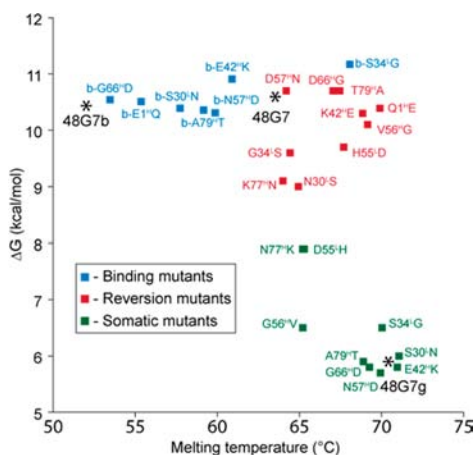


**Figure 4.** Scatter plot of binding energy  $\Delta G$  (kcal/mol) versus  $T_m$  (°C) of somatic mutations added to germline 48G7g (green), reversion mutations to mature 48G7 (red), and mutations to binding mutant 48G7b (blue). While most of the individual somatic mutants display similar binding affinities and thermal stabilities to that of 48G7g, each of the individual binding mutations (G56<sup>H</sup>V, N77<sup>H</sup>K, and D55<sup>L</sup>H) noticeably decreases stability while improving binding. Single-mutation variants of 48G7b all maintain high-binding affinity with greatly varying stabilities, with 48G7b-S34<sup>L</sup>G providing a significant increase in  $T_m$ . For exact values, see Tables S1 and S2, Supporting Information.

Interestingly, the three somatic mutations that decreased stability the most (D55<sup>L</sup>H, G56<sup>H</sup>V, and N77<sup>H</sup>K), as well as the somatic mutations that increased stability the most (S34<sup>L</sup>G, N57<sup>H</sup>D, and E42<sup>H</sup>K) are all located in the loops connecting the  $\beta$  strands, suggesting that the plasticity of these loops in germline structures not only facilitates evolution of binding affinity but also readily enhances stability during antibody maturation. We have now observed that somatic mutation and clonal selection optimize both antibody stability and affinity in three different germline antibodies, suggesting that this is likely a general phenomenon. Finally, we are currently investigating whether somatic mutations also affect protein folding, proteolytic stability, translation rates or trafficking to the cell surface and likewise affect the clonal selection process.

## ■ ASSOCIATED CONTENT

### 📄 Supporting Information

Supplemental material as described in text. This material is available free of charge via the Internet at <http://pubs.acs.org>.

## ■ AUTHOR INFORMATION

### Corresponding Author

magliery.1@osu.edu, fwang@calibr.org, schultz@scripps.edu

### Notes

The authors declare no competing financial interest.

## ■ ACKNOWLEDGMENTS

We thank Peter Lee and the Ian Wilson lab for the use of their ForteBio Octet RED96 for binding affinity measurements, and we also thank Virginia Seely for assistance with manuscript preparation. This work was supported by NIH Grant R01 GM062159 (PGS), The Skaggs Institute of Chemical Biology (PGS), and NIH Grant R01 GM083114 (TJM). This is manuscript #23062 of The Scripps Research Institute.

## ■ REFERENCES

- (1) French, D. L.; Laskov, R.; Scharff, M. D. *Science* **1989**, *244*, 1152–1157.
- (2) Kim, S.; Davis, M.; Sinn, E.; Patten, P.; Hood, L. *Cell* **1981**, *27*, 573–581.
- (3) Di Noia, J. M.; Neuberger, M. S. *Annu. Rev. Biochem.* **2007**, *76*, 1–22.
- (4) King, A. C.; Woods, M.; Liu, W.; Lu, Z.; Gill, D.; Krebs, M. R. H. *Protein Sci.* **2011**, *20*, 1546–1557.
- (5) Yin, J.; Beuscher, A. E., IV; Andryski, S. E.; Stevens, R. C.; Schultz, P. G. *J. Mol. Biol.* **2003**, *330*, 651–656.
- (6) Wedemayer, G. J.; Patten, P. A.; Wang, L. H.; Schultz, P. G.; Stevens, R. C. *Science* **1997**, *276*, 1665–1669.
- (7) Yin, J.; Mundorff, E. C.; Yang, P. L.; Wendt, K. U.; Hanway, D.; Stevens, R. C.; Schultz, P. G. *Biochemistry* **2001**, *40*, 10764–10773.
- (8) Schultz, P. G.; Yin, J.; Lerner, R. A. *Angew. Chem., Int. Ed.* **2002**, *41*, 4427–4437.
- (9) Wang, F.; Sen, S.; Zhang, Y.; Ahmad, I.; Zhu, X.; Wilson, I. A.; Smider, V. V.; Magliery, T. J.; Schultz, P. G. *Proc. Natl. Acad. Sci.* **2013**, *110*, 4261–4266.
- (10) Patten, P. A.; Gray, N. S.; Yang, P. L.; Marks, C. B.; Wedemayer, G. J.; Boniface, J. J.; Stevens, R. C.; Schultz, P. G. *Science* **1996**, *271*, 1086–1091.
- (11) Yang, P. L.; Schultz, P. G. *J. Mol. Biol.* **1999**, *294*, 1191–1201.
- (12) Chong, L. T.; Duan, Y.; Wang, L.; Massova, I.; Kollman, P. A. *Proc. Natl. Acad. Sci.* **1999**, *96*, 14330–14335.
- (13) Wedemayer, G. J.; Wang, L. H.; Patten, P. A.; Schultz, P. G.; Stevens, R. C. *J. Mol. Biol.* **1997**, *268*, 390–400.
- (14) Jacobs, J.; Schultz, P. G.; Sugawara, R.; Powell, M. J. *Am. Chem. Soc.* **1987**, *109*, 2174–2176.
- (15) Lavinder, J. J.; Hari, S. B.; Sullivan, B. J.; Magliery, T. J. *J. Am. Chem. Soc.* **2009**, *131*, 3794–3795.
- (16) NetNGlyc 1.0 Server. Center for Biological Sequence Analysis. <http://www.cbs.dtu.dk/services/NetNGlyc> (accessed Feb 5, 2013).
- (17) Ekiert, D. C.; Friesen, R. H. E.; Bhabha, G.; Kwaks, T.; Jongeneelen, M.; Yu, W.; Ophorst, C.; Cox, F.; Korse, H. J. W. M.; Brandenburg, B.; Vogels, R.; Brakenhoff, J. P. J.; Kompier, R.; Koldijk, M. H.; Cornelissen, L. A. H. M.; Poon, L. L. M.; Peiris, M.; Koudstaal, W.; Wilson, I. A.; Goudsmit, J. *Science* **2011**, *333*, 843–850.